

TSAMT: Time-Series-Analysis-based Motion Transfer among Multiple Cameras

Yaping Zhao^a, Guanghan Li^b, Haitian Zheng^c, and *Zhongrui Wang^a

^aThe University of Hong Kong

^bTsinghua University

^cThe University of Rochester

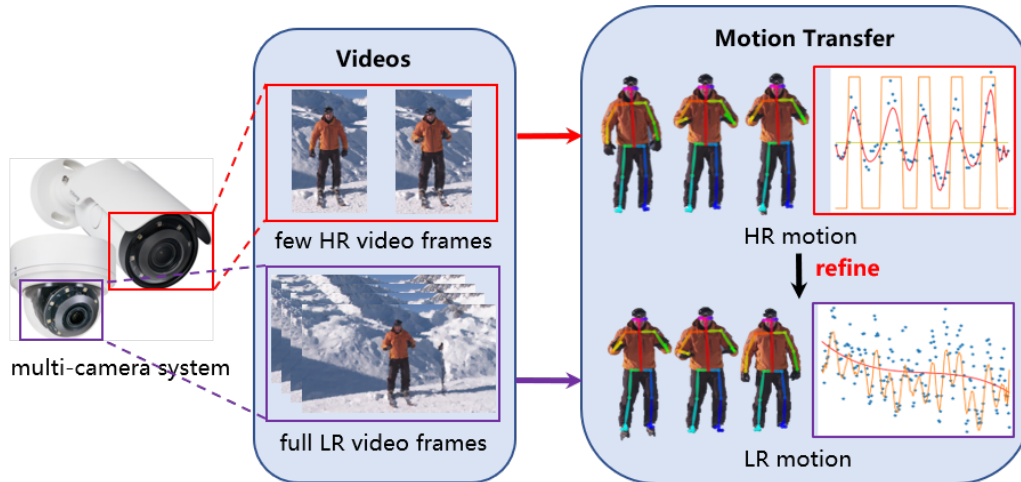


Figure 1. Using a multi-camera system, multi-scale human-centric videos could be obtained. After estimating 3D human poses from HR and LR videos, HR human motion patterns could be extracted, and transferred across cameras to enhance the inferior pose estimation on LR videos.

ABSTRACT

Along with advances in optical sensors is the common practice of building an imaging system with heterogeneous cameras. While high-resolution (HR) videos acquisition and analysis are benefited from hybrid sensors, the intrinsic characteristics of multiple cameras lead to an interesting motion transfer problem. Unfortunately, most of the existing methods provide no theoretical analysis and require intensive training data. In this paper, we propose an algorithm using time series analysis for motion transfer among multiple cameras. Specifically, we firstly identify seasonality in motion data, and then build an additive time series model to extract patterns that could be transferred across cameras. Our approach has a complete and clear mathematical formulation, thus being efficient and interpretable. Through quantitative evaluations on real-world data, we demonstrate the effectiveness of our method. Furthermore, our motion transfer algorithm could combine with and facilitate downstream tasks, *e.g.*, enhancing pose estimation on LR videos with inherent patterns extracted from HR ones. Code is available at <https://github.com/IndigoPurple/TSAMT>.

Keywords: Motion Transfer, Time Series Analysis, Multi-Camera Systems, Computational Imaging

1. INTRODUCTION

With the rapid development of optical sensors, multi-camera systems have become emerging solutions to computational imaging. For instance, by exploiting a short-focus lens to obtain large field-of-view (FoV) videos and long-focus ones to capture high-resolution (HR) local-view details, multi-camera systems^{1,2} can synthesize HR

*Zhongrui Wang is the corresponding author.



Figure 2. A case for surveillance and security, where a multi-camera system can observe pedestrian trajectories in a large FoV video. Meanwhile, the HR details of pedestrians are captured by local-view cameras. With such a setting, it is desirable to fuse the information from both global and local view, such that interested or suspicious objects can be recognize and the corresponding HR human details can be extracted.

video by embedding details into low-resolution (LR) video. Considering the most widely used multi-camera applications in our daily life, *e.g.*, smart city and live sports, it has become a popular practice to capture multi-scale human-centric videos via hybrid-camera systems. Along with those applications are demands for embedding human details into global-view videos. However, the fundamental issue remains, especially when dealing with a moving human body: how to transfer human motion across heterogeneous cameras.

Figure 2 showcases a surveillance and security setting, where a multi-camera system can observe pedestrian trajectories in a large FoV video. Meanwhile, the HR details of pedestrians are captured by local-view cameras. With such a setting, it is desirable to fuse the information from both global and local view, such that interested or suspicious objects can be recognize and the corresponding HR human details can be extracted. However, the inherent multi-scale characteristics of hybrid cameras, in terms of local spatial resolution, bring inevitable challenges to information fusion. Furthermore, due to the nonrigid motion of human bodies and poor pose estimation performance on LR videos, it is difficult to integrate the multi-scale human-centric videos into a single one that retains both large FoV and HR details.

To solve this problem, a recent work² proposed a motion analysis algorithm. After obtaining 3D human poses from HR and LR videos, HR human motions are transferred to enhance the inferior pose estimation on LR videos. Although they have successfully transferred human details among hybrid cameras, no mathematical formulation or theoretical analysis has been established for such an algorithm. On the other hand, with the development of deep learning, human motion transfer tends to use neural networks, which work in a black-box manner with less requirement on mathematical modeling. However, those learning-based methods require intensive training data and suffer from a long training time.

To improve the above-mentioned approach, we propose a motion transfer algorithm for multi-camera systems. Our approach has a complete and clear mathematical formulation and it does not require training data, thus being efficient and interpretable. We provide an algorithmic guarantee for motion transfer under the multi-camera setting. Specifically, our algorithm extracts the intrinsic motion patterns from human-centric videos and performs motion transfer tasks using time series analysis. Through quantitative evaluations on real-world data, we demonstrate the effectiveness of our method.

Our main contributions are listed as follows:

- We propose a time-series-analysis-based motion transfer algorithm for multi-camera systems, which has a complete and clear mathematical process.

- Our approach is interpretable and requires no training data. In comparison to learning-based methods, it provides an algorithmic guarantee and does not require the computationally exhausted training procedure.
- Experiments on real data demonstrate the effectiveness of our method. With our motion transfer algorithm, pose estimation on LR videos could be refined with intrinsic patterns extracted from HR ones.

2. RELATED WORK

2.1 Motion synthesis

There is a great amount of work in synthesizing human motion with controlled statistics.³⁻⁵ With statistical models and learned parameters, desired novel motions could be generated under manual control. However, the diversity of generated motion is limited with the variation in the training dataset.

2.2 Motion transfer

With the development of deep learning and neural networks, Villegas *et al.*^{6,7} utilized human pose for future frames prediction and human video synthesis. Ma *et al.*^{8,9} synthesized novel human videos given a reference image and a target pose. Siarohin *et al.*¹⁰ made a further step and proposed a deformable network architecture. Unfortunately, all of them are highly dependent on the training dataset and show degenerated performance when dealing with real data cases.

2.3 Time series analysis

Time series analysis¹¹⁻¹³ is widely used for numerous applications. For instance, geophysics uses it for marine seismic and multi-component streamer data analysis;¹⁴ remote sensing utilizes it for Landsat imagery processing;¹⁵ astronomy analyzes telescope observations with it;¹⁶ hydrology exploits it for analyzing streamflow and climate data;¹⁷ financial industries deal with the stock exchange and price series in daily stock market;¹⁸ in the medical field, it works for electroencephalogram and electrocardiogram signals processing.¹⁹

However, there exists little work using time series analysis for motion transfer among multiple cameras. Therefore, we propose a motion transfer algorithm for multi-camera systems using time series analysis, especially seasonality analysis.^{20,21}

3. METHOD

Under our multi-camera setting, after obtaining 3D human poses from HR and LR videos, we propose an algorithm that refines the LR pose sequence θ^L based on time series analysis, especially seasonality analysis. The key insight behind this is that most human actions are approximately repetitive, such as walking, running, physical exercise, *etc.* In other words, some kinds of human motion data in HR and LR videos have seasonality.

The overall motion transfer works as follows: 1) identify seasonality; 2) build an additive time series model; 3) find periodic points; 4) extract additive factor; and 5) transfer motion pattern. We choose the $\theta_{1,1}$ as an example, which represents the 1_{th} axis-angle of the 1_{th} joint in the SMPL model²² (the ankle joints of a human body). Figure 3(a) illustrates an example of normalized $\theta_{1,1}$ values in a walking sequence with 80 HR frames, and Figure 3(b) represents values from 200 LR frames.

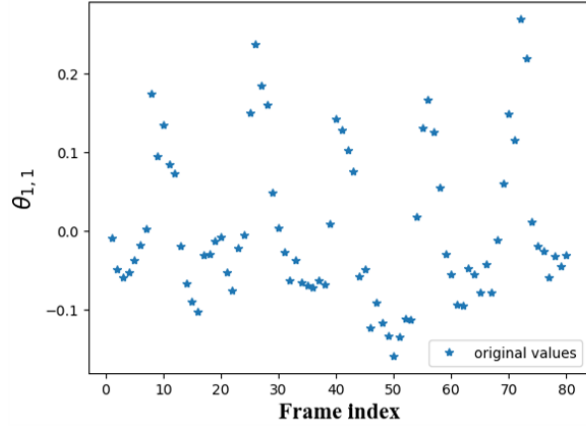
3.1 Seasonality identification

First, auto-correlation function (ACF)²³ is utilized to identify the cyclicity of HR motion data. As illustrated in Figure 4(a), the curve performs periodic variation with maximal value of a function during predefined intervals, and gradually decreases to zero.

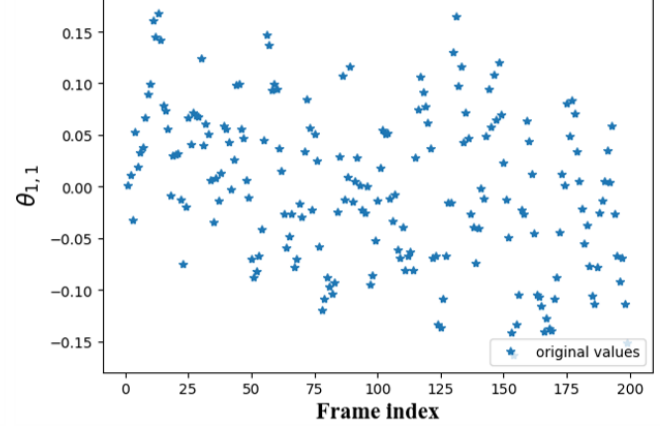
Although the human motion is regularly repetitive, the length of a period is usually unfixed but around a constant value, denoted as “reference period” l , which can be estimated using Fourier analysis:

$$l = n/f, \quad (1)$$

where n is the total frame number of the motion sequence, and f is the frequency with the strongest response. Figure 4(b) shows the Fourier series of the HR motion data, we can see that $f = 5$ has the strongest response, so its reference period is: $80/5 = 16$.

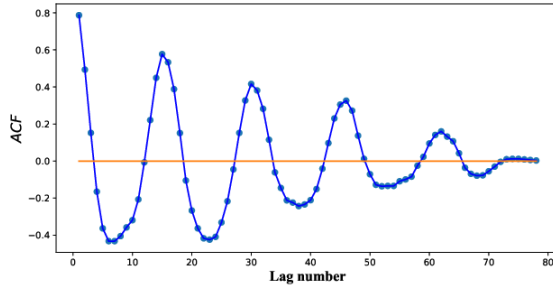


(a)

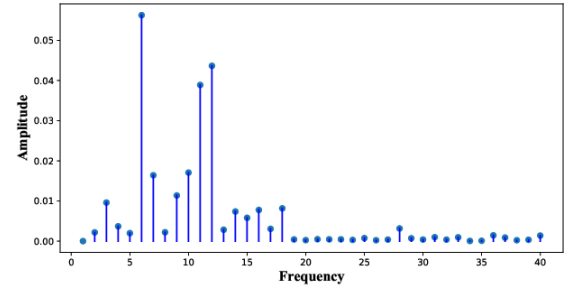


(b)

Figure 3. HR and LR motion data. (a) and (b) represent the $\theta_{1,1}$ value of the HR and LR motion data, respectively.

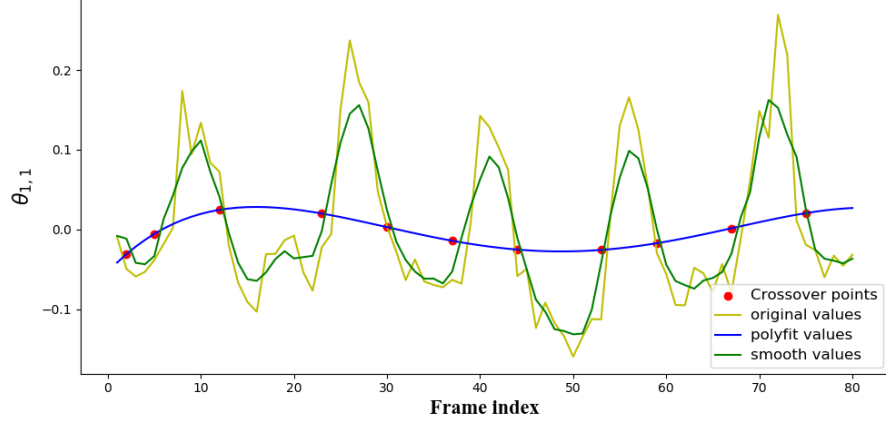


(a)

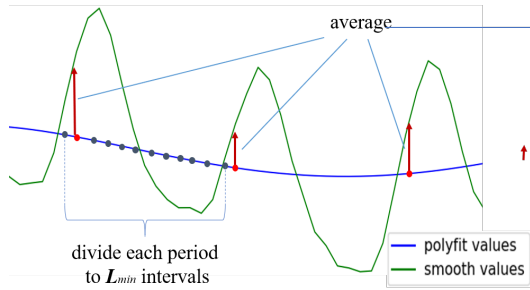


(b)

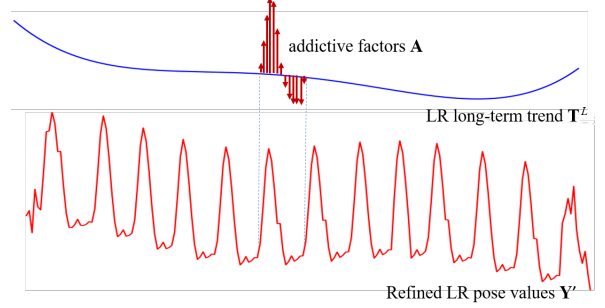
Figure 4. (a) Auto-correlation result of HR motion data. It performs periodic variation with the maximal value of a function during predefined intervals and gradually decreases to zero. (b) In the Fourier series of the HR motion data, we can see that $f = 5$ has the strongest response, so its reference period is: $80/5 = 16$.



(a)



(b)



(c)

Figure 5. (a) Crossover points location. The periods could be located by finding the crossover points of the blue and dark green curves, shown as red circles. (b) To refine LR pose values with HR ones, we estimate the additive factor \mathbf{A} by averaging all the periods. (c) To refine LR pose values with HR ones, we add back the additive factor to the long-term trend \mathbf{T}^L to generate the final refined LR poses.

3.2 Addictive time series model

Next, we build an additive time-series model²⁴ to decompose LR pose values into reasonable components, which is defined as:

$$\mathbf{Y} = \mathbf{S} + \mathbf{T} + \mathbf{E}, \quad (2)$$

where \mathbf{Y} represents the original pose values; \mathbf{S} represents the short-term variation; \mathbf{T} represents the long-term trend; and \mathbf{E} denotes the noise. We estimate the long-term trend of the LR sequence by the polynomial fitting of pose values based on the least-square method:

$$\mathbf{T}^L = c_0 + c_1 \theta_{1,1}^L + c_2 (\theta_{1,1}^L)^2 + \cdots + c_{n-1} (\theta_{1,1}^L)^{n-1} + c_n (\theta_{1,1}^L)^n, \quad (3)$$

where \mathbf{T}^L denotes the long-term trend of the LR sequence; c_0, \dots, c_n are constant parameters; $\theta_{1,1}^L$ denotes the $\theta_{1,1}$ value of the LR data. The order n of this fitting function is determined as the highest one that ensures: $1^{-10} < |c_n| < f$, where c_n is the coefficients of the highest-order item, f is the amount of periods in a pose value sequence.

3.3 Periodic points location

Next, we first smooth pose values with moving average to reduce the disturbance of noise. After that, the periods can be located by finding the crossover points of the original and polynomial fitting value curves, shown as red circles in Figure 5(a).

To remove the unreasonable period indices, we only preserve the indices with the period within $[0.8l, 1.2l]$. Then, we estimate the additive factors²⁵ \mathbf{A} by averaging all the periods, and add back to the long term trend \mathbf{T} to generate the final refined LR poses, as shown in Figure 5(b) and Figure 5(c).

More specifically, We find frame indices corresponding to the crossover points of the smooth pose curve and the long-term trend curve. Since we work on discrete series instead of continuous ones, we find the \pm sign changes of the difference between the two series. However, due to non-ideal polynomial fitting, the estimate of \mathbf{T} might have slight fluctuation to overfit the head and tail values in pose sequence. So we utilize the reference period l to remove unreasonable period indices. Specifically, for every periodic index p , we examine its validity by checking the existence of a neighbor periodic index p' that satisfies:

$$\begin{aligned} p' &= \arg \min_{p'} |p' - p|, \\ \text{s.t. } ||p' - p| - l| &< (1 - \alpha) \times l, \end{aligned} \quad (4)$$

where α is confidence, we set $\alpha = 80\%$; l is the reference period. That is to ensure each of the periodic points p has a neighbor periodic point p' with their distance within the confidence interval.

3.4 Additive factor extraction

After finding periods in time series, we calculate the minimum period number l_{min} of HR and LR sequences, and divide each period into l_{min} intervals as evenly as possible. Then, to extract the additive factor for motion pattern transfer, based on Equation 2, we eliminate the long-term trend component from the HR pose values by:

$$\mathbf{A} = \mathbf{Y}^H - \mathbf{T}^H = \mathbf{S}^H + \mathbf{E}^H, \quad (5)$$

where \mathbf{A} is the additive factor, *i.e.*, difference between the original pose \mathbf{Y}^H and the long-term trend \mathbf{T}^H . And it consists of short-term variation \mathbf{S}^H and the noise component \mathbf{E}^H .

Using Equation 5, we could extract the periodically repetitive pattern \mathbf{A} for motion transfer, as shown in Figure 5(b). Since the additive factor \mathbf{A} in each period varies, we use the mean value of all periods to perform motion transfer in a comprehensive manner. Therefore, we infer mean additive factor $\bar{\mathbf{A}} = (\bar{a}_1, \dots, \bar{a}_i, \dots, \bar{a}_l)$ as:

$$\bar{a}_j = \frac{\sum_{i=1}^n \mathbb{1}\{\phi(i) = j\} a_i}{(f \times m)}, \quad a_i \in \mathbf{A}, \quad (6)$$

where a_i is the i_{th} value of the additive factor \mathbf{A} , specifically for the i_{th} interval in a period; f is the amount of periods; m is the amount of values in the i_{th} interval; ϕ is a correspondence function that identify frame index i of the time series is within the j_{th} interval of a period:

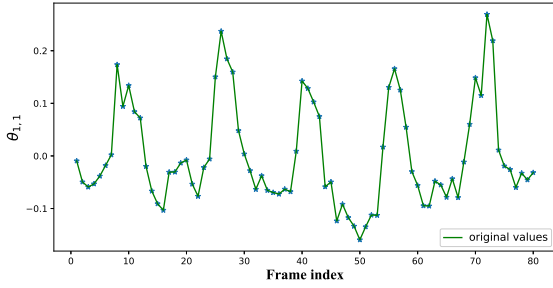
$$\phi(i) = j. \quad (7)$$

3.5 Pattern transfer

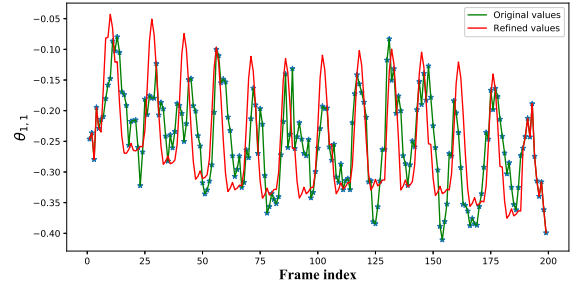
Finally, we add the additive factors $\bar{\mathbf{A}}$ to the LR long-term trend T^L , to enforce it fit to the regular patterns extracted from the HR motion sequence, as shown in Figure 5(c). The refined LR pose values $\mathbf{Y}' = (y'_1, \dots, y'_i, \dots, y'_n)$ is calculated as:

$$y'_i = t_i + \bar{a}_{\phi(i)}, \quad (8)$$

where y'_i is the i_{th} value of the refined LR pose; t_i is the i_{th} value of the LR long-term trend \mathbf{T}^L .



(a)



(b)

Figure 6. HR and LR motion data. (a) and (b) represent the $\theta_{1,1}$ value of the HR and LR motion data, respectively.



Figure 7. Performance on human detail synthesis across heterogeneous cameras. Top: the synthesized results without our motion transfer method. Bottom: the synthesized results with our method. Without motion transfer, there are intensive jitters on the head and legs.

4. EXPERIMENT

To verify the performance of our algorithm, we apply it to the real data captured by a dual-camera system.² Given few HR video frames and full LR video frames, we first perform pose estimation using OpenPose,²⁶ to obtain pose value sequences. As the green curves in Figure 6 show, the estimated pose sequence of the HR video is of high quality, while that of the LR one suffers severe noise. However, with our motion transfer method, the LR pose values could be refined, as shown in Figure 6(b). Our results preserve the long-term trend in the LR pose sequence, and successfully transfer the motion pattern from the HR sequence to enhance the LR data quality.

To make a further step in evaluating our motion transfer method, we combine it with a downstream vision task, embedding HR human details into LR videos. Specifically, on the top of Figure 7, without the help of our algorithm, the results of direct human detail synthesis look weird. For instance, we observe obvious jittering due to the blurring frames, especially on the head and legs. The feet even appeared in extremely unnatural poses. In contrast, benefit from motion transfer, the results in the bottom row of Figure 7 substantially eliminate the motion jittering.

5. CONCLUSION

In this paper, we propose an algorithm using time series analysis for motion transfer among multiple cameras. Our approach has a complete and clear mathematical formulation and it does not require any training data, thus being efficient and interpretable. Through quantitative evaluations on real-world data, we demonstrate the effectiveness of our method. Furthermore, our method could be extended to deal with various kinds of motions and thus is not limited to dealing with human-centric videos.

REFERENCES

- [1] Yuan, X., Fang, L., Dai, Q., Brady, D. J., and Liu, Y., “Multiscale gigapixel video: A cross resolution image matching and warping approach,” in *[2017 IEEE International Conference on Computational Photography (ICCP)]*, 1–9, IEEE (2017).
- [2] Li, G., Zhao, Y., Ji, M., Yuan, X., and Fang, L., “Zoom in to the details of human-centric videos,” in *[2020 IEEE International Conference on Image Processing (ICIP)]*, 3089–3093, IEEE (2020).
- [3] Chai, J. and Hodgins, J. K., “Constraint-based motion optimization using a statistical dynamic model,” in *[ACM SIGGRAPH 2007 papers]*, 8-es (2007).
- [4] Min, J. and Chai, J., “Motion graphs++ a compact generative model for semantic motion analysis and synthesis,” *ACM Transactions on Graphics (TOG)* **31**(6), 1–12 (2012).
- [5] Lau, M., Bar-Joseph, Z., and Kuffner, J., “Modeling spatial and temporal variation in motion data,” *ACM Transactions on Graphics (TOG)* **28**(5), 1–10 (2009).
- [6] Villegas, R., Yang, J., Zou, Y., Sohn, S., Lin, X., and Lee, H., “Learning to generate long-term future via hierarchical prediction,” in *[international conference on machine learning]*, 3560–3569, PMLR (2017).
- [7] Villegas, R., Yang, J., Ceylan, D., and Lee, H., “Neural kinematic networks for unsupervised motion retargeting,” in *[Proceedings of the IEEE Conference on Computer Vision and Pattern Recognition]*, 8639–8648 (2018).
- [8] Ma, L., Jia, X., Sun, Q., Schiele, B., Tuytelaars, T., and Van Gool, L., “Pose guided person image generation,” *arXiv preprint arXiv:1705.09368* (2017).
- [9] Ma, L., Sun, Q., Georgoulis, S., Van Gool, L., Schiele, B., and Fritz, M., “Disentangled person image generation,” in *[Proceedings of the IEEE Conference on Computer Vision and Pattern Recognition]*, 99–108 (2018).
- [10] Siarohin, A., Sangineto, E., Lathuiliere, S., and Sebe, N., “Deformable gans for pose-based human image generation,” in *[Proceedings of the IEEE Conference on Computer Vision and Pattern Recognition]*, 3408–3416 (2018).
- [11] CLEVELAND, W., “Analysis and forecasting of seasonal time series,” (1973).
- [12] Box, G. E. and Jenkins, G. M., “Time series analysis. forecasting and control,” in *[Holden-Day Series in Time Series Analysis, Revised ed., San Francisco: Holden-Day, 1976]*, (1976).
- [13] Brown, R. G., *[Smoothing, forecasting and prediction of discrete time series]*, Courier Corporation (2004).
- [14] Ghaderpour, E., Liao, W., and Lamoureux, M. P., “Antileakage least-squares spectral analysis for seismic data regularization and random noise attenuation,” *Geophysics* **83**(3), V157–V170 (2018).
- [15] Ahmed, M. R., Hassan, Q. K., Abdollahi, M., and Gupta, A., “Introducing a new remote sensing-based model for forecasting forest fire danger conditions at a four-day scale,” *Remote Sensing* **11**(18), 2101 (2019).
- [16] Ghaderpour, E. and Ghaderpour, S., “Least-squares spectral and wavelet analyses of v455 andromedae time series: The life after the super-outburst,” *Publications of the Astronomical Society of the Pacific* **132**(1017), 114504 (2020).
- [17] Veiga, V. B., Hassan, Q. K., and He, J., “Development of flow forecasting models in the bow river at calgary, alberta, canada,” *Water* **7**(1), 99–115 (2015).
- [18] Chakrabarty, A., De, A., Gunasekaran, A., and Dubey, R., “Investment horizon heterogeneity and wavelet: Overview and further research directions,” *Physica A: Statistical Mechanics and its Applications* **429**, 45–61 (2015).
- [19] Bhattacharyya, A., Sharma, M., Pachori, R. B., Sircar, P., and Acharya, U. R., “A novel approach for automated detection of focal eeg signals using empirical wavelet transform,” *Neural Computing and Applications* **29**(8), 47–57 (2018).
- [20] Hylleberg, S., *[Modelling seasonality]*, Oxford University Press (1992).
- [21] Wallis, K. F., “Seasonal adjustment and relations between variables,” *Journal of the American Statistical Association* **69**(345), 18–31 (1974).
- [22] Loper, M., Mahmood, N., Romero, J., Pons-Moll, G., and Black, M. J., “Smpl: A skinned multi-person linear model,” *ACM transactions on graphics (TOG)* **34**(6), 1–16 (2015).
- [23] Plosser, C. I., “Short-term forecasting and seasonal adjustment,” *Journal of the American Statistical Association* **74**(365), 15–24 (1979).

- [24] Maravall, A. and Pierce, D. A., “A prototypical seasonal adjustment model,” *Journal of Time Series Analysis* **8**(2), 177–193 (1987).
- [25] Yar, M. and Chatfield, C., “Prediction intervals for the holt-winters forecasting procedure,” *International Journal of Forecasting* **6**(1), 127–137 (1990).
- [26] Cao, Z., Hidalgo, G., Simon, T., Wei, S.-E., and Sheikh, Y., “Openpose: realtime multi-person 2d pose estimation using part affinity fields,” *IEEE transactions on pattern analysis and machine intelligence* **43**(1), 172–186 (2019).